Distribution of Avalanches in Interfacial Motion in a Porous Medium

Andrew Dougherty and Nathan Carle

Dept. of Physics, Lafayette College, Easton, PA 18042–1782

(April 13, 2000)

Abstract

We report measurements of the dynamics of an air/water interface moving through a model porous medium made of glass beads packed in a horizontal Hele-Shaw cell. At low flow rates, the interface does not move uniformly. Instead, some small regions move while others stay pinned, at least for a short time. The burst of motion when a pinned region breaks free is called an avalanche. In several theoretical models, such avalanches were found to follow a power-law distribution. In contrast, we find that even for very slow flow (capillary number $\mu U/\gamma \sim 2 \times 10^{-7}$) the number of avalanches of size s decays roughly exponentially with s.

64.60.Lx, 47.55.Mh

I. INTRODUCTION

When an interface is driven through a disordered medium, both the static shape and the dynamics of the motion can show considerable complexity. Common examples of this include the motion of domain walls in disordered magnetic systems [1], flux lines in superconductors [2], and imbibition in a random porous medium [3–9].

For the case of imbibition to be considered here, a viscous wetting fluid (water) displaces a non-viscous non-wetting fluid (air) in a random porous medium made from glass beads. The viscosity ratio ensures that the interface is nominally stable, but the randomness in the porous medium can still lead to a wrinkling of the interface.

One common approach to describe the behavior is to consider the interface velocity as a function of the applied pressure. The velocity is sometimes assumed to follow a scaling law of the form $v \sim (p/p_c - 1)^{\theta}$, where p_c is the critical pressure, below which the interface remains pinned. If the pressure is slightly above p_c, then some portions of the interface can advance, while others will tend to remain pinned. Since the pressure at a site can depend both on the externally applied pressure and on the local configuration or curvature, sites that were previously pinned may subsequently break free and move ahead in a sudden burst of motion, or avalanche.

One of the important advances in recent years is the exploration of the relation between the statistical properties of the interface near the pinning threshold and the properties of directed percolation clusters [6,10]. In addition, there has been considerable progress in grouping apparently dissimilar models and experiments into just a small number of universality classes [11–14]. These connections lead to many predictions for both the spatial and temporal scaling behavior of the interface.

Experimental measurements of these scaling properties can be quite difficult, though considerable progress has been made [3,8,9,15–17]. For example, in a finite system, there is no single global p_c. Instead, the minimum pressure required for the interface to move can vary from location to location during the course of the experiment. Thus there is no unique

functional relationship between v and p.

However, one feature that is common to nearly all of the models is that the interface moves in bursts, or avalanches, that have a power-law distribution in size. For reviews, see Refs. [18,19].

In this paper, we present measurements of the avalanches observed as water displaces air in a porous medium composed of glass beads packed in a thin, horizontal Hele-Shaw cell. Instead of a power-law distribution, we find a roughly exponential distribution of avalanche sizes.

II. EXPERIMENTS

The experiments were performed in a thin rectangular Plexiglas cell $125 \times 41 \times 0.16$cm. The porous medium was made of glass beads $170 \pm 20\mu$m in diameter, so that the thickness of the cell corresponds to approximately 9 beads. Prior to use, the beads were washed, rinsed thoroughly, dried, and sieved to remove any clumps. The cell was then tilted upright and placed on a shaker table. The beads were poured very slowly into the cell while it was being agitated. The net result was a fairly uniform packing of the beads; at least no large-scale packing anomalies were observed. We also performed some experiments with larger (360μm) beads but it was more difficult to ensure uniform packing, so those results are not included here.

Water was injected from a series of small holes in a tube aligned along one of the narrow ends of the cell. This approximately mimicked the ideal case of uniform injection along a line. The water was pumped by a syringe pump at a nominally constant rate.

Images were recorded with a charge coupled device (CCD) camera onto video tape. Only the central 17 cm of the system was recorded to avoid edge effects. The video tape was later digitized with a Data Translation DT2862 image processor with a spatial resolution of 512×480 pixels, and an intensity range of 0–255. The overall scale was approximately 271μm/pixel, or about 1.5 beads/pixel.

A typical image is shown in Fig. 1. The water is the dark region and is moving upwards. The average speed of the interface is 13.7μm/s, which corresponds to approximately 0.08 beads/s.

The motion of the interface is illustrated in Fig. 2, where the interface position is shown at 100-second intervals. All distances are in units of the bead diameter. Overall, the interface is fairly smooth and does not exhibit any significant overhangs. The large-scale curvature evident in Fig. 2 changes slowly only over a long time scale.

III. AVALANCHES

In order to characterize the avalanches, we computed the absolute value of the difference between image intensities of two images taken a fixed time Δt apart. A typical difference image for Δt =4s is shown in Fig. 3. Regions in the image where the water has moved show up as bright; regions where nothing happened are dark.

The activity is not spread uniformly along the interface, but is concentrated in small "bursts" or avalanches. Note, however, that none of the avalanches seems particularly large, nor are there many large dark regions where nothing happens. Instead, the activity seems to be spread fairly uniformly across the interface.

In order to quantify the sizes of the avalanches, we perform the following steps. First, we define an intensity threshold c for difference images such that only pixels with an intensity difference $\geq c$ are considered as "active" sites. Next, we group sets of connected nearest-neighbor active sites into distinct avalanches and record the horizontal and vertical sizes and the total area of each avalanche. Finally, we repeat this for all the difference images obtained. In practice, the vertical size of the avalanches shows little variation, so the measurements below will focus on the the total avalanche area s.

The normalized distribution of avalanche sizes $N(s)$ is shown on both semi-log and log-log scales in Fig. 4 for $c = 12$ and $\Delta t = 6$ (top), 4, and 2s (bottom). The distribution $N(s)$ is not well-described by a power law. After an initial rapid decrease, $N(s)$ decays approximately

exponentially over a reasonably wide range of avalanche sizes. At the largest sizes, however, the decay is slower than exponential. We can include that initial rapid decrease by modeling $N(s)$ by a power law with an exponential cut-off of the form $N(s) \sim s^{-b}e^{-s/L}$. For Δt=4s and c=12, the length scale L is approximately 55 bead diameters, and the power law exponent b is approximately 0.3, but these values vary with both Δt and c.

A. Dependence on Analysis Parameters

The exact numerical values obtained for L and b depend on the values used for both c and Δt.

As is evident from Fig. 4, the characteristic length L increases as the time difference Δt between images is increased. This general behavior is rather easy to understand. The interface velocity v is approximately 0.08 beads/s, so it takes about 12s for the interface to advance a distance of 1 bead. If the interface advanced completely uniformly, then in the span of 12s there would be a single "avalanche" 1 bead high spanning the entire image. Such an avalanche would have a total area of 1570 (in units of the bead diameter squared). For the shorter time intervals Δt considered here, the pump only supplies enough water for a maximum avalanche size of $\Delta t/12$ of that area. Further, since the interface moves in a number of places at once, rather than in just a single avalanche, the characteristic length scale L is only a fraction of the maximum possible avalanche size.

In an attempt to minimize this effect, we have examined the behavior as Δt gets larger, but we still did not see evidence of emergent power-law behavior. Instead, the small avalanches observed at lower Δt appear to simply merge horizontally together until each "avalanche" is a single mostly-horizontal cluster spanning the system.

In particular, we noted that most avalanches were only a few beads in height. We also never noted any regions of the interface that stayed pinned for a long time. These features are illustrated in Fig. 5, where we show the difference images for Δt values ranging from 2s (bottom) to 12s (top). Note that the vertical extent of the avalanches changes only slightly;

the avalanches spread out mostly in the direction parallel to the interface.

There is also a potential problem that can arise as larger values of Δt are considered, namely the merging of distinct avalanches [20]. This is particularly evident in Fig. 5. To check whether such merging significantly affected our measurements of $N(s)$, we performed simulations of a version of the paper-wetting model of Buldyrev *et al.* [6].

In this model, a fraction p of the sites of a rectangular array is filled with "pinning" sites; the remaining sites are empty. Initially, all the sites in the bottom row are filled, so the initial interface is just a horizontal line. The simulation then proceeds in two stages at each time step. First, all empty sites adjacent to a filled site are filled. Second, all overhangs are eroded.

The results for $N(s)$ are shown on semi-log and log-log scales in Fig. 6 for $\Delta t = 1$, 2, 4, and 6 simulation time steps. As Δt is increased, we do observe that many smaller avalanches appear to combine, but we still find power law behavior at large s. Thus while merging of individual small avalanches will affect the small s regime, it does not change the overall scaling from power law to exponential. [21].

The characteristic length L of the experimental results also increases as the cut-off c is decreased, since a smaller change in intensity is now counted as an active site. This will pick up regions in the image where the water has not yet fully invaded a site (*i.e.* it is not filled in the third dimension yet). This effect is evident in Fig. 7, which shows the distribution of avalanche sizes for Δt=4s with intensity cutoffs c ranging from 8 (top) to 18 (bottom).

From visual inspection of the images, $c = 12$ seems to strike the best balance between rejecting noise in the image and preserving as much structure as possible, but none of the qualitative results are particularly sensitive to the precise cutoff value used.

The dependence of the fitted length scale L on the analysis parameters is summarized in Fig. 8(a) for Δt =2, 4, and 6s, and intensity cutoffs ranging from 8 (top) to 18 (bottom).

Similarly, the fitted power law exponent b also varies somewhat with the analysis parameters, though it always remains small. This is shown in Fig. 8(b) for the same conditions.

IV. DISCUSSION

Ideally, we might only expect to observe power-law avalanche behavior in the limit $v \to 0$. However, power law scaling of interfacial shapes and dynamics has been widely reported in other porous media experiments [3–9], even though they were also typically performed at finite velocities. Further, experiments at velocities significantly slower than that used here would take prohibitively long (though see Ref. [8] for extremely slow velocities). We did, however, try running with a velocity of $4v$, and observed no qualitative changes in the distribution of avalanches.

An additional potential problem with even slower velocities is the use of a mechanical syringe pump, which itself can be subject to stick/slip motion. This motion might mask the motion of the interface. To test for such problems, we ran the experiment with a pressure reservoir instead of a syringe pump. That is, we had the syringe pump fill a reservoir at a constant flow rate, and had the reservoir connected to the experimental apparatus via a siphon. Again, we observed no qualitative changes in the results.

The exponential behavior we observe is probably most similar to that reported by Furuberg, Maloy, and Feder [16] in experiments on slow drainage, which is the opposite of the process of imbibition considered here. In that work, they measured an exponential distribution of pressure jumps, instead of a power-law distribution. The authors hypothesized that the incompressibility of water causes the capillary pressure at the interface to decrease abruptly during a burst, and this tends to dampen the further spreading of the avalanche. However, they were able to identify groups of jumps that would become a single "composite" burst in a sufficiently large system. They were also able to show that these composite bursts followed a power law distribution.

It remains to be seen whether a similar analysis is possible for our data. However, if this is indeed an important effect in these experiments, then it does seem unlikely that simply going to slower velocities will change the distribution to a power law.

In conclusion, we have performed direct measurements of the avalanche distribution

during the interfacial motion in imbibition in a model porous medium. Instead of the power law distribution commonly found in some models, we have found a roughly-exponential distribution of avalanche sizes.

ACKNOWLEDGMENTS

Some equipment used in this work was obtained through a Joseph H. DeFrees grant of Research Corporation. A.D. also thanks A.-L. Barabási and P.-z. Wong for helpful conversations.

REFERENCES

[1] N. Martys, M. Robbins, and M. Cieplak, Phys. Rev. B **44**, 12294 (1991).

[2] S. Bhattacharya and M. J. Higgins, Phys. Rev. Lett. **70**, 2617 (1993).

[3] M. A. Rubio, C. A. Edwards, A. Dougherty, and J. P. Gollub, Phys. Rev. Lett. **63**, 1685 (1989).

[4] S. He, G. Kahanda, and P. z. Wong, Phys. Rev. Lett. **69**, 3731 (1992).

[5] V. H. Horváth, F. Family, and T. Vicsek, J. Phys. A **24**, L25 (1991).

[6] S.V. Buldyrev, A.-L. Barabási, F. Caserta, S. Havlin, H.E. Stanley and T. Vicsek, Phys. Rev. A **45**, R8313 (1992).

[7] V. Horváth and H. Stanley, Phys. Rev. E **52**, 5166 (1995).

[8] T. Delker, D. Pengra, and P. Wong, Phys. Rev. Lett. **76**, 2902 (1996).

[9] T. Kwon, A. E. Hopkins, and S. E. O'Donnell, Phys. Rev. E **54**, 685 (1996).

[10] L. Tang and H. Leschhorn, Phys. Rev. A **45**, R8309 (1992).

[11] L. A. N. Amaral, A.-L. Barabási, and H. E. Stanley, Phys. Rev. Lett. **73**, 62 (1994).

[12] L. A. N. Amaral, A.-L. Barabási, H. A. Makse, and H. E. Stanley, Phys. Rev. E **52**, 4087 (1995).

[13] L. Tang, M. Kardar, and D. Dhar, Phys. Rev. Lett. **74**, 920 (1995).

[14] The present experiments have been shown to be in the isotropic universality class. See Réka Albert, Albert-László Barabási, Nathan Carle, and Andrew Dougherty, to be published.

[15] V. K. Horváth, F. Family, and T. Vicsek, Phys. Rev. Lett. **67**, 3207 (1991).

[16] L. Furuberg, K. J. Maloy, and J. Feder, Phys Rev E **53**,966 (1996).

[17] V. K. Horváth, F. Family, and T. Vicsek, Phys. Rev. Lett. **65**, 1388 (1990).

[18] M. Paczuski, S. Maslov, and P. Bak, Phys. Rev. E **53**, 414 (1996).

[19] S.V. Buldyrev, L.A.N. Amaral, A.-L. Barabási, S.T. Harrington, S. Havlin, J. Kertesz, R. Sadr-Lahijany and H.E. Stanley, Fractals **4**, 307 (1996).

[20] For a more extensive discussion of overlapping avalanches, see Terence Hwa and Mehran Kardar, Physical Review A **45**, 7002 (1992).

[21] One potential complication is that the paper-wetting model is in the anisotropic universality class [11–13], while the present experiments are in the isotropic universality class [14]. We also considered the Leschhorn model discussed in [Heiko Leschhorn, Physica A, **195**, 324, (1993)], which is in the isotropic class. However, our simulations of that model did not show clear evidence of a power-law distribution of avalanches for any value of Δt.

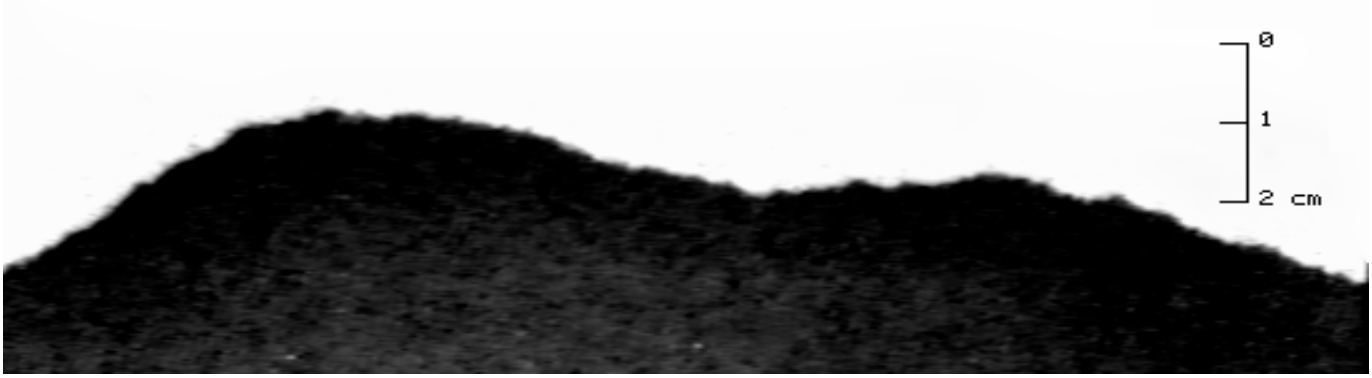

FIG. 1. Typical interface. The water is the dark region and is moving upwards at an average speed of v= 13.7μm/s. The scale bar shows 1cm intervals.

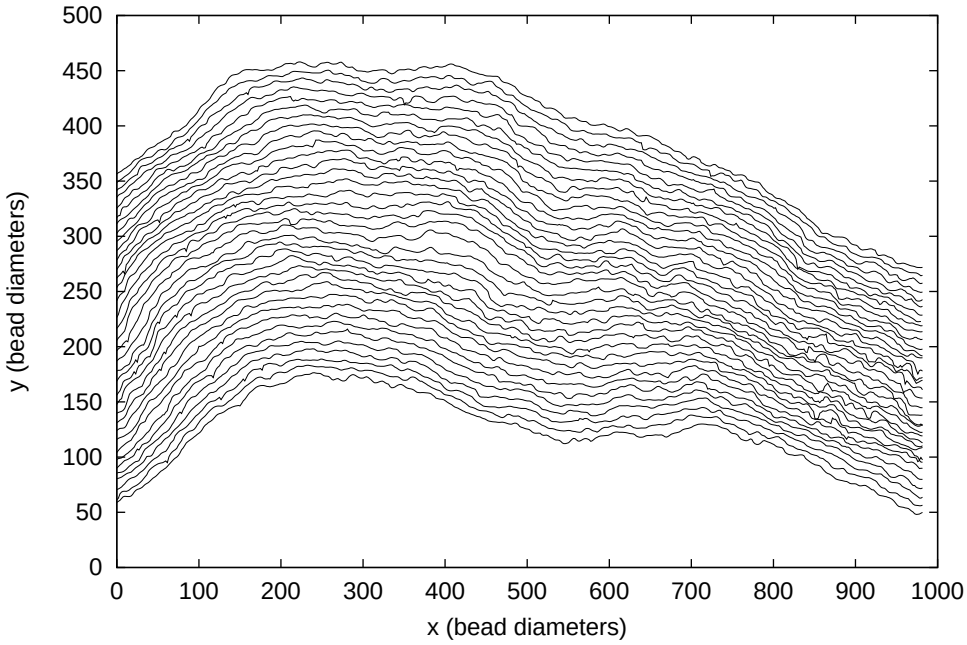

FIG. 2. Interface positions taken at 100-second intervals. All distances are in units of the bead diameter. The water enters at the bottom and is moving upward.

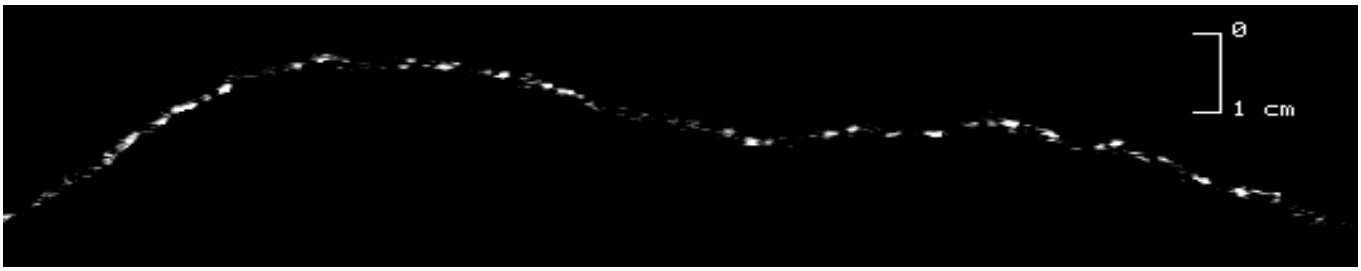

FIG. 3. Image showing the absolute value of the difference between two images taken 4 seconds apart. Bright regions show where the interface has moved. The contrast in the image has been significantly enhanced to bring out details. The scale bar indicates 1cm.

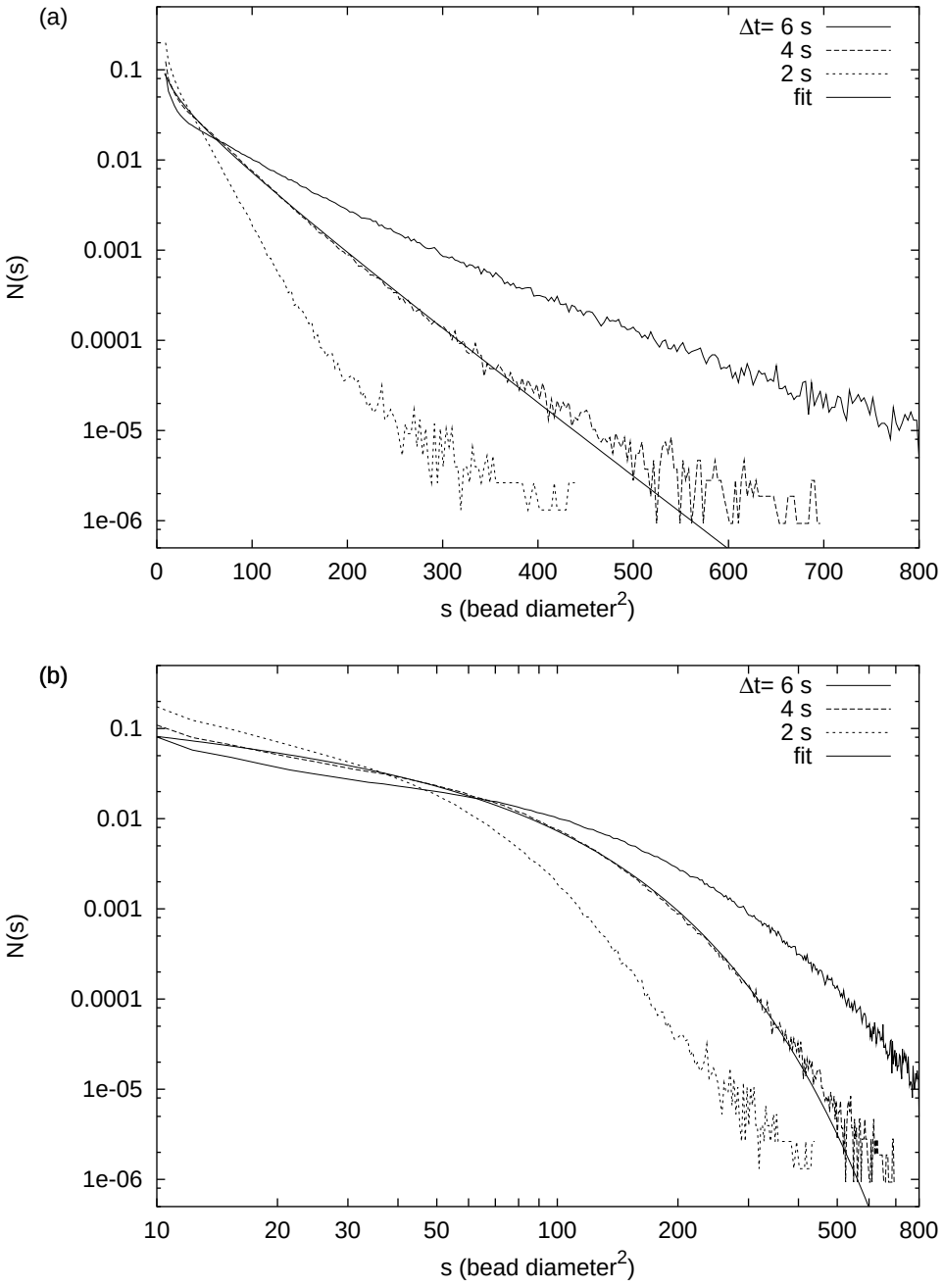

FIG. 4. Distribution of avalanche sizes on semi-log (a) and log-log (b) scales for $c = 12$ and Δt =6 (top), 4 (middle) and 2s (bottom). The solid line is a fit to $N(s) \sim s^{-b} e^{-s/L}$ for Δt =4s.

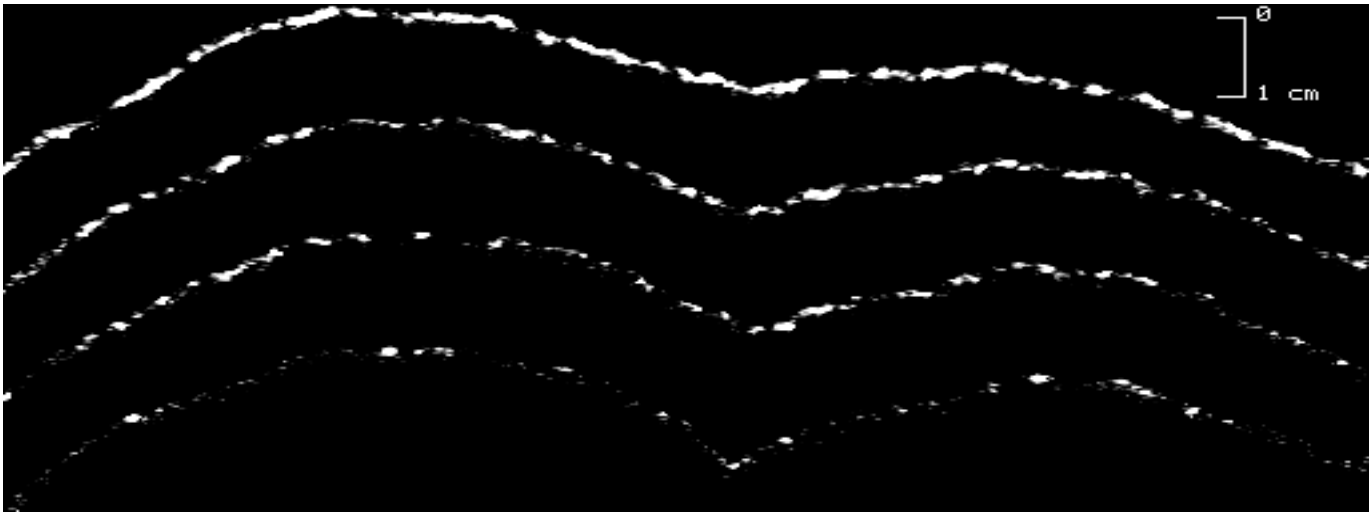

FIG. 5. Difference images for Δt =2 (bottom), 4, 8, and 12s (top). The scale bar indicates 1 cm.

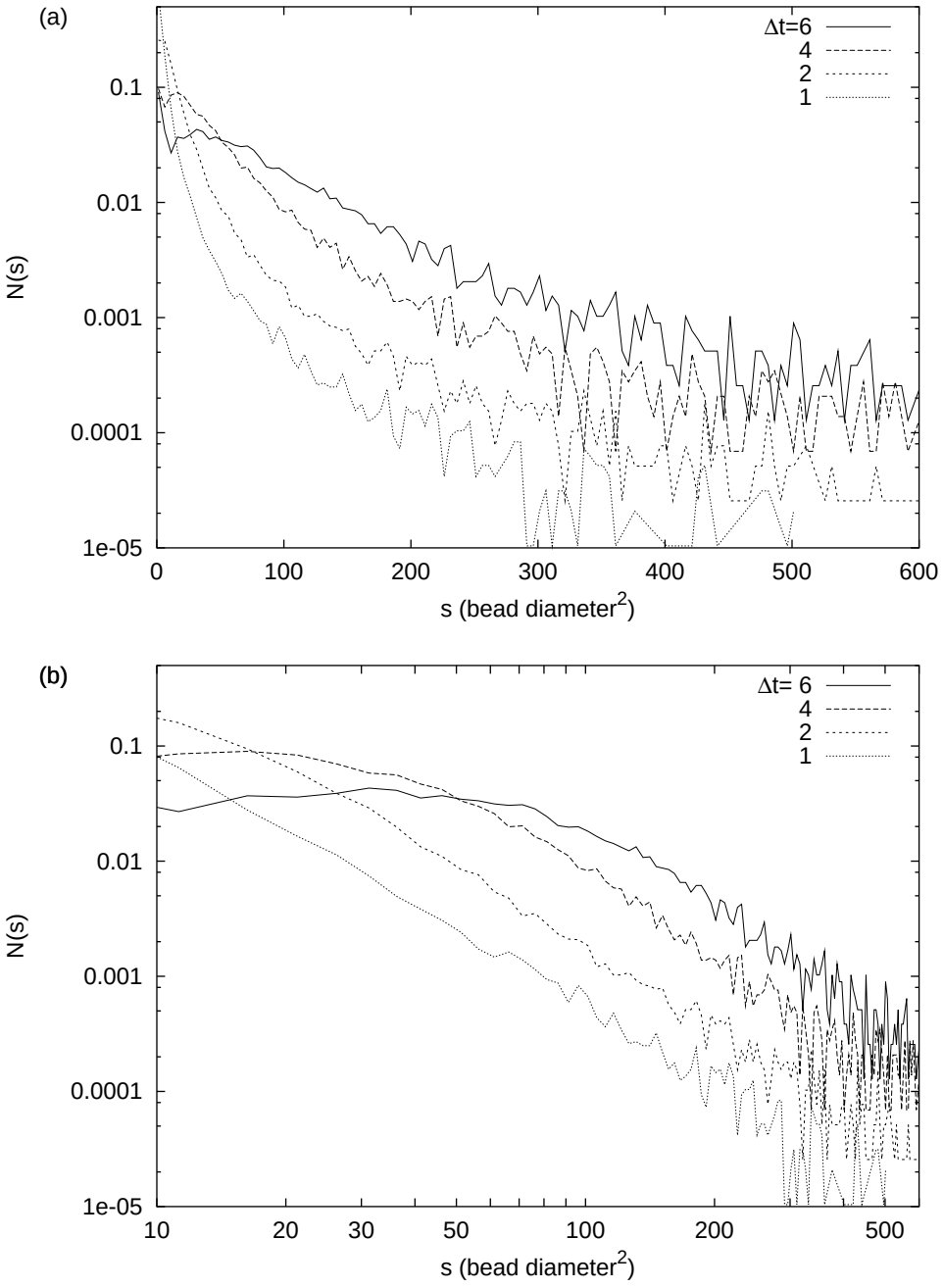

FIG. 6. Avalanche distribution for paper-wetting simulations on semi-log (a) and log-log (b) scales for Δt =6 (top), 4, 2, and 1 (top) timestep.

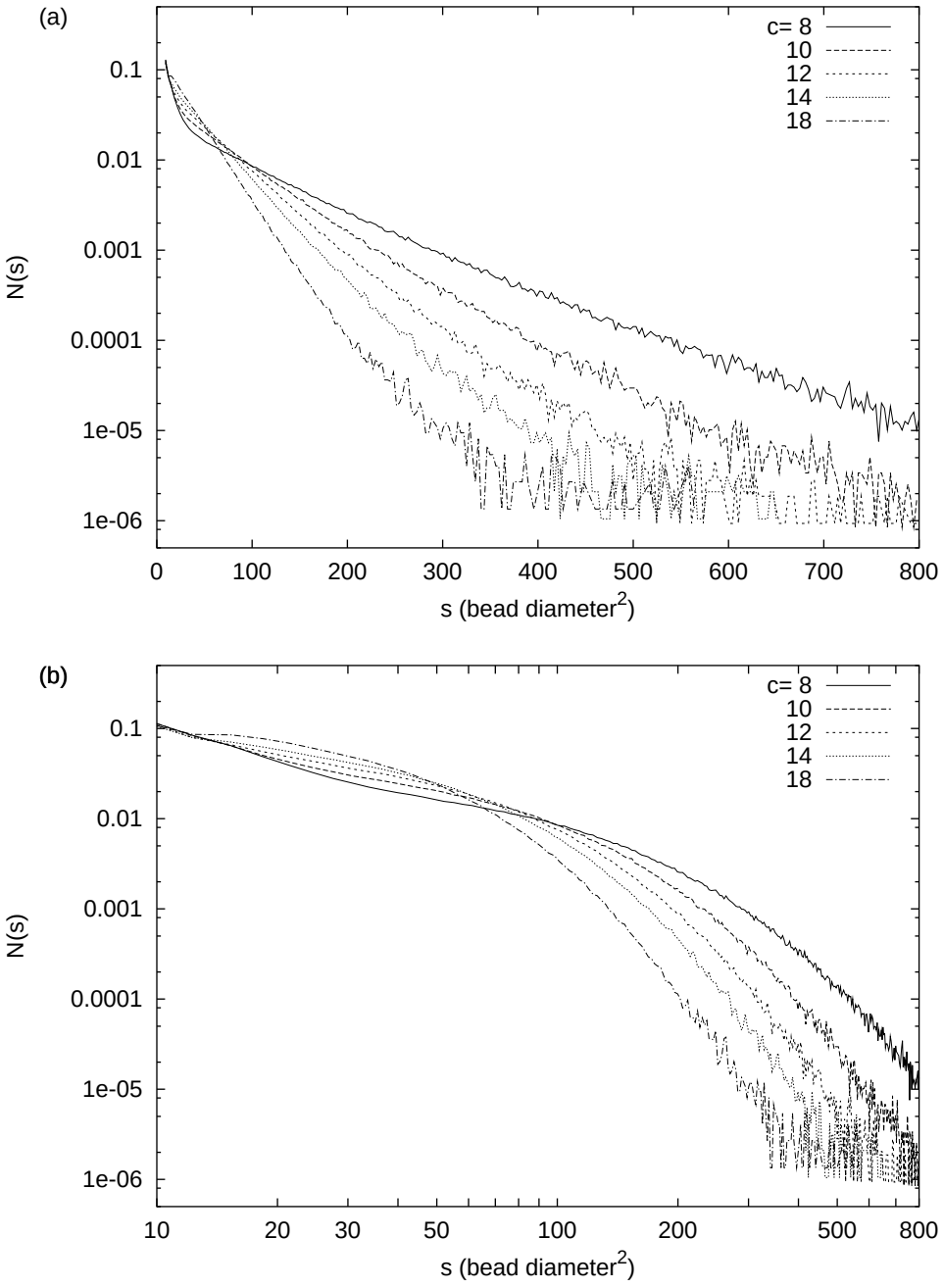

FIG. 7. Distribution of avalanche sizes shown on semi-log (a) and log-log (b) scales for $\Delta t = 4s$ and intensity cutoffs c ranging from 8 (top) to 18 (bottom).

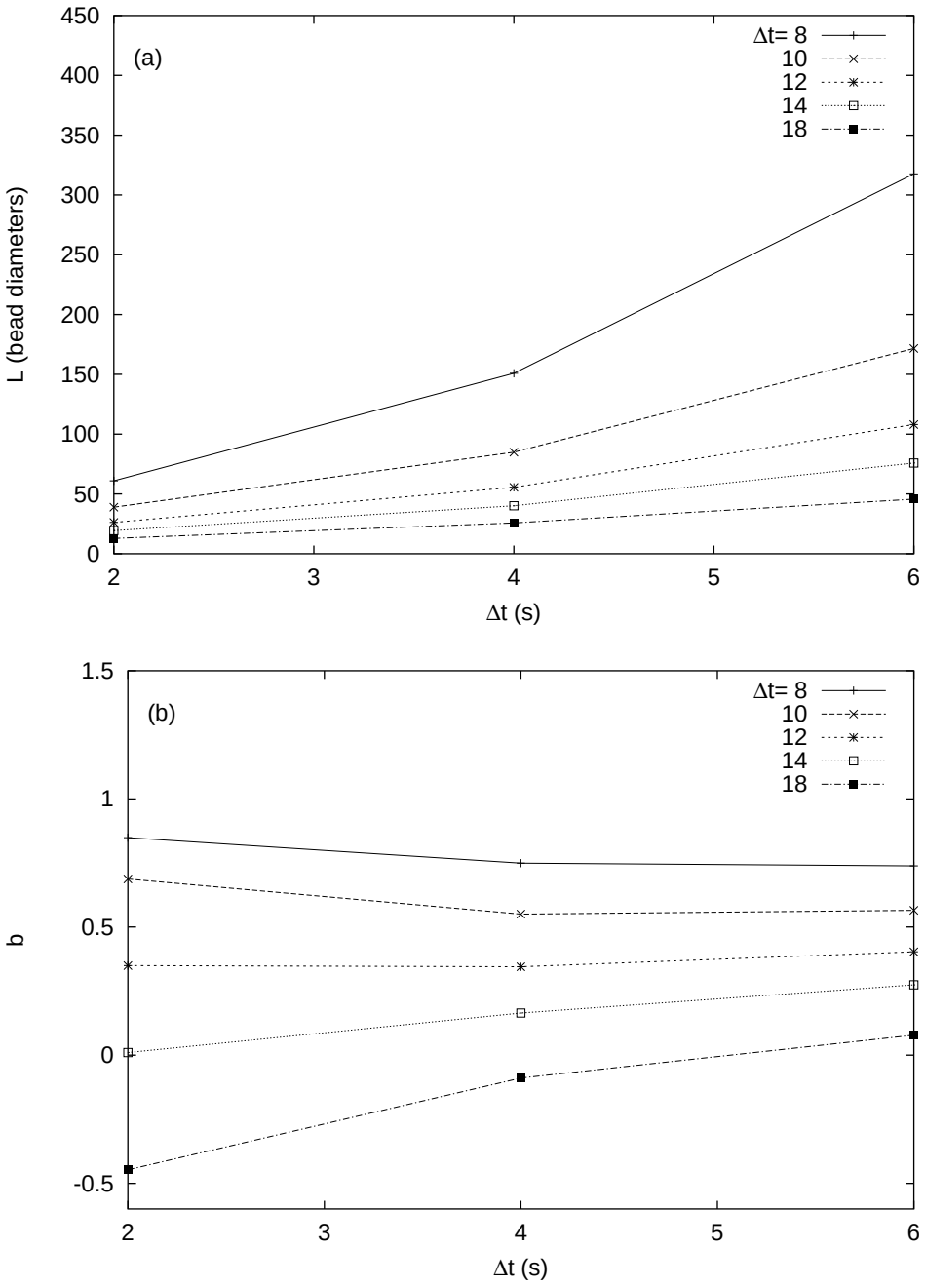

FIG. 8. Dependence of characteristic length L (a) and power law exponent b (b) on Δt for intensity cutoffs c ranging from 8 (top) to 18 (bottom).